

Characteristics of Rapidly Formed Hydrogen-Producing Granules and Biofilms

Zhen-Peng Zhang,^{1,2} Sunil S. Adav,³ Kuan-Yeow Show,⁴ Joo-Hwa Tay,^{1,2}
David Tee Liang,² Duu-Jong Lee,³ Ay Su⁵

¹School of Civil and Environmental Engineering, Nanyang Technological University, Singapore, Singapore

²Institute of Environmental Science and Engineering, Nanyang Technological University, Singapore, Singapore

³Department of Chemical Engineering, National Taiwan University, Taipei, Republic of China

⁴Faculty of Engineering and Science, University of Tunku Abdul Rahman, 31900 Kampar, Perak, Malaysia; telephone: 603-41079802; fax: 603-41079803;

e-mail: kyshow2003@yahoo.com.sg

⁵Department of Mechanical Engineering, Fuel Cell Center, Yuan-Ze University, Taoyuan, Republic of China

Received 24 January 2008; revision received 14 April 2008; accepted 21 April 2008

Published online 2 May 2008 in Wiley InterScience (www.interscience.wiley.com). DOI 10.1002/bit.21956

ABSTRACT: The physicochemical and microbiological characteristics of rapidly formed hydrogen-producing granules and biofilms were evaluated in the present study. Microbial species composition was examined using the 16S rDNA-based separation and sequencing techniques, and spatial distribution and internal structure of microbial components were evaluated by examining the confocal laser scanning microscope (CLSM) images. Phylogenetic analysis indicated that a pure culture of *Clostridium pasteurianum*-like bacterium (98% similarity) was found in microbial community of granules and biofilms. It is postulated that containing such a species favored the rapid immobilization of hydrogen-producing culture. Manure granules and biofilms secreted 24–35 mg extracellular proteins and 142–175 mg extracellular polysaccharides in each gram of culture (in VSS). Such a high productivity of extracellular polymers (ECP), a bio-glue to facilitate cell-to-cell and/or cell-to-substratum interaction, may work as the driving forces for the immobilization of *C. pasteurianum*. As abundant proteins were noted in the granule cores, it can be derived that rapid formation of the hydrogen-producing granules could be due to the establishment of precursor protein-rich microbial nuclei.

Biotechnol. Bioeng. 2008;101: 926–936.

© 2008 Wiley Periodicals, Inc.

KEYWORDS: biohydrogen production; granule; biofilm; confocal laser scanning microscope (CLSM); phylogenetic analysis; protein core

Introduction

Hydrogen production technologies have attracted worldwide attention in recent years. This is largely due to the soaring concerns on environmental deterioration and sustainability derived from the utilization of conventional fossil fuels and on the potential of hydrogen as an ideal alternative. Biological hydrogen production using fermentative, photosynthetic bacteria, or algae is an environmentally friendly and energy saving process, and might be a promising alternative to the conventional fossil fuels-based hydrogen production processes. The feasibility of anaerobic hydrogen production from organic wastes has been widely demonstrated by numerous research groups in different countries all over the world (Wu et al., 2006; Zhang et al., 2006, 2008b).

Recently, granule- and biofilm-based systems have widely been used for anaerobic hydrogen production since they are more capable of maintaining higher biomass concentration and could operate at high dilution rates without biomass washout (Fang et al., 2002; Show et al., 2007; Zhang et al., 2007c, 2008a). It is generally believed that spontaneous biofilm formation or granulation of hydrogen-producing bacteria can occur with reduced HRT in upflow column reactors or continuous stirred tank reactors (CSTRs) (Fang et al., 2002; Oh et al., 2004; Yu and Mu, 2006). A long startup period of a few months, however, is needed for complete development of those bioparticles (Fang et al., 2002; Yu and Mu, 2006). For example, during the startup of an upflow

anaerobic sludge blanket (UASB) hydrogen-producing reactor, Mu and Yu (2006) found that small granules were formed with diameters of 0.4–0.5 mm at the reactor bottom until 140 days of operation which developed rapidly to 2.0 mm after 60 more days. A long period of 86 days was also required to form hydrogen-producing biofilms on the support matrix in a thermal trickling biofilter (Oh et al., 2004).

A novel approach to accelerate granulation of hydrogen-producing sludge was developed by our research group (Zhang et al., 2007a,b). Applying acid incubation on the culture demonstrated an ability to initiate microbial granulation of sludge within 3–5 days in a CSTR or an anaerobic fluidized bed reactor (AFBR). Changing the culture pH resulted in improvement in surface physico-chemical properties of the culture favoring microbial granulation. The improvement included the reduced surface charge numbers, and the enhanced cell hydrophobicity and extracellular proteins/polysaccharides ratio. Rapid formation of biofilms was able to be achieved in the AFBR as the same seed sludge was inoculated without the acid incubation (Zhang et al., 2007a). Although characteristics of hydrogen-producing granules were previously assessed (Fang et al., 2002; Mu and Yu, 2006), characteristics knowledge of those rapidly formed granules and biofilms is not reported yet. To grasp a better understanding on the mechanisms involved in the cell immobilization of hydrogen-producing cultures, the present work elucidated the physicochemical and microbiological properties of the hydrogen-producing granules and biofilms. Microbial community of the hydrogen-producing granules and biofilms was examined using the 16S rDNA-based techniques, and spatial distribution and internal structure of microbial components were evaluated by examining the confocal laser scanning microscope (CLSM) images.

Materials and Methods

Experimental Approach

The granules were cultivated in either a CSTR (6 L, working volume) or an AFBR (1.4 L, working volume). Both reactors were operated at a constant temperature of 37°C and fed with 10 g-glucose/L glucose-based synthetic wastewater containing mineral elements as described previously (Zhang et al., 2006). The reactors were seeded with the acclimated sludge which had been cultivated with glucose (10 g-glucose/L) by stepwise HRT reduction from 50 to 6 h in an CSTR at pH 5.5 (Zhang et al., 2006) before use for cell immobilization. After the inoculation, the microbial culture was subject to an acid incubation for 24 h by shifting the culture pH from 5.5 to 2.0. The culture was resumed to pH 5.5 after the 24-h incubation and then fed with synthetic wastewater mainly consisting of glucose continuously at HRTs of 12–0.5 h for an 8-month operation of CSTR and a 2-month operation of AFBR. Detailed description on the

reactors configuration and operation can be found in our recent studies (Zhang et al., 2007a,b). Granules were harvested from the CSTR and the AFBR for examination at a HRT of 0.5 h.

Cultivation of the biofilms was carried out in another identical AFBR with granular activated carbon (GAC) as the support carriers whose physical characteristics had been presented in a previous study (Zhang et al., 2007c). The biofilm AFBR was operated under the same conditions as the granule AFBR except that the acclimated sludge was not subject to the acid incubation. Biofilms were sampled for examination at a HRT of 0.5 h.

Biogas and Effluent Analysis

All reactors were designed as closed system. They were flushed with argon gas for 10 min to create an anaerobic environment before startup. Amount of biogas produced was recorded daily, either by using water displacement method for the AFBRs or by a wet gas meter (Ritter TG 05, Germany) for the CSTR. The biogas composition with respect to H₂, CO₂ and CH₄ was analyzed by a gas chromatography. Detailed procedures for measurement of biogas amount and composition had been described in the previous work (Zhang et al., 2006, 2007b). Glucose concentration was determined following the phenol-sulfuric acid method reported by Dubois et al., (1956). Measurements of suspended solids (SS) and volatile suspended solids (VSS) were performed according to the Standard Methods (APHA, 1998).

Physical and Physicochemical Characteristics Analysis

The microbial compositions and structure of granules and biofilms were observed qualitatively with a scanning electron microscope (SEM) (Stereoscan 420; Leica Cambridge Instruments, Cambridge, UK). The bioparticle samples were gently washed with distilled water and allowed to settle naturally. The bioparticles were then fixed with 2% glutaraldehyde for 4 h. The fixed samples were washed with 0.1 M sodium cacodylate buffer for 3 times and left for 20 min each time, and dehydrated by successive passages through 50, 70, 85, 95% ethanol and stored in 100% ethanol. The dehydrated particles were then transferred to a Critical Points Dryer (E3000, VG Microtech, East Grinstead, West Sussex, UK) where samples were immersed in liquid CO₂ phase instead of original dehydrating agent for 1 h. Thereafter, the samples were dried at 36–38°C and a pressure of 1,200 psi. The dried samples were sputtered coat with Au-Pd (SPI-Module Sputter coater, Structure Probe, West Chester, PA), and finally observed by SEM. The sizes and morphologies of granules and biofilms were analyzed by using an image analysis system (Quantimet 500 Image Analyzer; Leica Cambridge Instruments, Cambridge, UK). The settling velocities of granules determined with 30 replicate samples ($n = 30$) or biofilms ($n = 30$) in water

were measured by recording the time taken for an individual granule or biofilm to fall from a certain height (1.0 m) in a measuring cylinder (10 cm in diameter; 1.5 m in height).

ECP was extracted using formaldehyde–NaOH method following the procedures reported previously (Liu and Fang, 2002). The ECP was analyzed for total carbohydrates and proteins which are dominant components typically found in extracted ECP (Liu and Fang, 2002; Schmidt and Ahring, 1996). Carbohydrate concentration was determined according to the colorimetric procedure of Dubois et al. (1956) using glucose for the calibration curve. Protein content was measured using bovine serum albumin as the standard according to the modified Lowry procedure of Peterson (Protein Assay Kit No. P5656-Sigma Aldrich, St. Louis, MO) described previously (Aquino and Stuckey, 2003).

16S rDNA-Based Microbial Analysis

The DNA from the granules and biofilm were extracted via enzymatic lysis using extraction buffer (100 mM Tris–HCl at pH 8.0, 100 mM EDTA at pH 8.0, and 1.5 M NaCl) containing Proteinase K (10 mg mL^{−1}, Amresco Inc., Solon, OH) (Adav et al., 2007). Samples were incubated in a 15 mL polypropylene tube at 37°C for 30 min and shaken at 150 rpm (Orbital shaker water bath, Deng Yng, Taichung, Taiwan). The sodium dodecyl sulfate (SDS) was added (20%) to samples and incubated at 65°C for 90 min. Samples were subjected to 2 cycles of freeze-thawing. The supernatant was collected after centrifugation at 6,000g for 10 min, and the aqueous phase was extracted with phenol: chloroform: isoamyl alcohol (25:24:1, v:v:v). The DNA was precipitated utilizing isopropanol and pelleted by centrifugation (10,000g) for 10 min, then resuspended in water.

Different sets of forward/reverse primer pairs (969F/1393R, 67F/1512R, and 27F/1512R, see Table I) were used for the amplification of 16S rDNA sequences to double check the species composition of the microbial community. Primer pairs 63F/1512R and 27F/1512R were used to amplify complete sequences of approximately 1,400–1,485 base pairs as primers 969F/1393R amplified short sequence of 430–440 base pairs. The PCR mixture consisted of 5 µL PCR buffer (10×), 2.5 µL MgCl₂ (25 mM), 2.5 µL dNTP (2.5 mM), 0.25 µL (100 mM) each of the primer solutions, 0.5 µL Taq. Polymerase (Promega, Madison, WI), 100 ng of DNA template and ddH₂O to make 50 µL. PCR reaction

mixture composition was the same for all PCR reactions. The PCR reactions including both forward and reverse primers and template DNA were performed with an eppendorf mastercycler (Eppendorf AG, Hamburg, Germany) by following an initial denaturation at 94°C for 3 min, 30 or 35 touchdown thermal cycles, and a final extension at 72°C for 7 min (Table I).

DNA fragments were separated by denaturing gradient gel electrophoresis (DGGE) according to the methods described by Muyzer et al. (1993). Only a single band was identified in DGGE profile of the PCR-amplified DNA with three sets of primer pairs, representing the DNA fragments from an individual bacterium. The PCR-amplified DNA with the primer set of 27F and 1512R was sequenced using the ABI Prism model 3730 (version 3.2) DNA sequencer (Applied Biosystems, Foster City, CA).

Analysis of DNA sequences and homology searches were completed with standard DNA sequencing programs, and the BLAST server of National Centre for Biotechnology Information (NCBI) using the BLAST algorithm. The obtained DNA sequences and their closest 16S rDNA sequences of reference microorganism retrieved from the Ribosomal Database Project (Maidak et al., 2000) were aligned manually with the software Bioedit (Hall, 1999) to construct phylogenetic tree using the neighbor-joining (NJ) method. Relative support for particular clades in the NJ tree topologies was estimated by using 500 replicates of the bootstrap procedure, performed with the Phylip software package (Felsenstein, 1989).

The nucleotide sequences reported in the present work have been submitted to the GenBank, EMBL, and DDBJ databases and assigned the following accession numbers: EF656615 AB308401 (AFBR-B), EF656616 AB308402 (AFBR-G), and EF656617 AB308403 (CSTR-G).

Staining and CLSM Imaging

The collected bioparticles were maintained in a fully hydrated state during staining. Calcofluor white (Sigma Aldrich, St. Louis, MO) was used to stain the β-D-glucopyranose polysaccharides. The fluorescein isothiocyanate (FITC) (Molecular Probes, Carlsbad, CA) is an amine reactive dye that stains proteins and other amine-containing compounds such as amino-sugars in the bioparticles. Nile Red (Molecular Probes) is a phenoxazine dye that was utilized to stain lipids.

Table I. Primers and PCR program conditions used for 16S rDNA genes amplification.

Primer pair	Sequence (5′–3′)	PCR program		
		Initial denaturation	Touchdown thermal cycle	Final extension
968F ^a , 1393R	AACGCGAAGAACCTTAC; ACGGAGGTAGCTGTCTGACATGA	94°C, 3′	94°C, 30″; 54°C, 55″; 72°C, 90″ (30 cycles)	72°C, 7′
63F; 1512R	CAGGCCTAACACATGCAAGTC; ACGGCTACCTTGTTACGACT	94°C, 3′	94°C, 45″; 55°C, 60″; 72°C, 90″ (35 cycles)	72°C, 7′
27F; 1512R	AGAGTTTGATCMTGGCTCAG ^b ; ACGGCTACCTTGTTACGACT	94°C, 3′	94°C, 40″; 55°C, 60″ 72°C, 120″ (35 cycles)	72°C, 7′

^aGC clamp of 40 base pairs (5′-CGCCCGGGGCCCCGGGCGGGGCGGGGCACGGGGGG-3′) was attached to 968F primer.

^bM = C:A in equal proportion.

Fluorescently labeled lectins Concanavalin A-tetramethylrhodamine conjugate (Molecular Probes) were used to bind to α -mannopyranosyl and α -glucopyranosyl sugar residues. As Con A can also bind with protein and glycoconjugate groups associated with cell walls, SYTO 63 (Molecular Probes), which is a cell wall-permeable nucleic acid stain, was used to differentiate the cells. The SYTOX blue (Molecular Probes), a cell wall-impermeable stain, was applied to stain the dead cells in the bioparticles.

The staining scheme was proposed as follows: The SYTO 63 (20 μ M, 100 μ L) was first dripped on the sample and then placed on a shaker table for 30 min. Next, 0.1 M sodium bicarbonate buffer (100 μ L) was added to the sample to keep amine group in non-protonated form; then, the FITC solution (10 g/L, 10 μ L) was added to the sample for 1 h at room temperature. Finally, the Con A solution (0.2 g/L, 100 μ L), Nile Red (10 mg/L, 100 μ L) and calcofluor white (300 mg/L, 100 μ L) were applied to the sample for 30 min in series followed by SYTOX Blue (2.5 μ M, 100 μ L). After each of the six staining stages described above, the sample was washed twice to remove excess stain using phosphate-buffered saline (PBS). The stained bioparticles were embedded and frozen at -20°C , from which 40- μ m sections were cut using a cryomicrotome and mounted on microscopic slides for observation. The details on staining and CLSM are available elsewhere (Chen et al., 2007a,b).

Confocal laser scanning microscopy (CLSM; Leica TCS SP2 Confocal Spectral Microscope Imaging System, GmbH, Wetzlar, Germany) was employed to probe the internal structure of granules and biofilms. The bioparticles were imaged using a 10 \times or 20 \times objective and analyzed using Leica confocal software (Leica TCS SP2 Confocal Spectral Microscope Imaging System, GmbH). The fluorescence of calcofluor white was detected by excitation at 400 nm and from the emission width at 410–480 nm (blue). The FITC probe was detected by excitation at 488 nm and emission at 500–550 nm (green). Excitation at 543 nm and emission at 550–600 nm (light blue) were used to detect Con A conjugates. The fluorescence of SYTO 63 (red) was determined from excitation at 633 nm and emission at 650–700 nm. The fluorescent intensity of SYTOX Blue (pink) was detected via excitation at 458 nm and emission at 460–500 nm. Excitation and emission wavelength were set at 514 nm and 625–700 nm for the detection of fluorescein Nile Red (yellow).

Results

Hydrogen Production Performance

The acclimated hydrogen-producing bacteria were immobilized by forming granules in a CSTR and AFBRs and forming biofilms in the AFBRs with GAC as support carriers (Zhang et al., 2007a,b). Restated, formation of granules in the CSTR and AFBR was accomplished in a very short period of 3–5 days after the acclimated sludge was subject to

an acid incubation for 24 h by shifting the culture pH from 5.5 to 2.0, which was much shorter than the formation times of several months required under normal conditions in other studies (Fang et al., 2002; Yu and Mu, 2006). Use of support media as starting nuclei may result in rapid formation of biofilms without acidification within 36 h.

The ability of granules and biofilms to convert glucose into hydrogen in terms of hydrogen yield ranged from 1.66 to 1.81 mol-H₂/mol-glucose, while hydrogen production ability of the biomass (specific hydrogen production rate, mmol-H₂/g-VSS h) was in a range of 8.31–8.96 mmol-H₂/g-VSS h (Table II). The reactor performance such as glucose conversion rate and volumetric hydrogen production rate of granules and biofilms had been presented previously (Zhang et al., 2007a,b).

Physical and Physicochemical Characteristics

Physical and physicochemical characteristics of hydrogen-producing granules and biofilms are summarized in Table III. The CSTR and AFBR granule sizes (in Sauter mean diameter) ranged from 0.2 to 4.2 mm (average 1.7 ± 0.9 mm, $n \geq 100$) and from 0.2 to 3.5 mm (1.5 ± 0.3 mm, $n \geq 100$), respectively. The sizes of biofilm particles ranged from 1.0 to 2.6 mm averaging at 1.8 ± 0.4 mm ($n \geq 100$). The thickness of biofilms was estimated to be in a range of 0.3–1.5 mm. Bioparticle morphology was expressed in terms of roundness, and the roundness of CSTR granules, AFBR granules and AFBR biofilms were 2.6 ± 1.4 ($n \geq 100$), 1.3 ± 0.5 ($n \geq 100$), and 1.6 ± 0.6 ($n \geq 100$), respectively. Larger values of roundness indicated for the granules cultivated in the CSTR might be attributed to the fact that some scattered granules were found in the CSTR, which were not granules in the real sense and thus called as “patch flocs” in the context. In contrast to the sphericity or sphericity-like of healthy granules, those patch flocs were in irregular shapes as shown in Table III. The CSTR and AFBR hydrogen-producing granules had settling velocities of 13–69 m/h and 21–78 m/h in water, respectively, while the settling velocities of biofilms were 58–189 m/h, due to the presence of much heavier support cores.




The granules and biofilms consisted mainly of volatile organic materials as the ash contents were found to be $2.5 \pm 0.5\%$ ($n = 12$) for the CSTR granules, $8.6 \pm 1.0\%$ ($n = 12$) for the AFBR granules and $9.2 \pm 1.0\%$ ($n = 12$) for the AFBR biofilms, respectively (Table III). The low ash

Table II. Hydrogen production performance of granules and biofilms.

Culture type	H ₂ yield (mol-H ₂ /mol-glucose)	Specific H ₂ production rate (mmol/g-VSS h)
CSTR-granule	1.81	8.31
AFBR-granule	1.66	8.77
AFBR-biofilm	1.71	8.96
Acclimated sludge ^a	1.88	15.62

^aReferred to a previous work by Zhang et al. (2006).

Table III. Physical characteristics of hydrogen-producing granules and biofilms.

	CSTR-granule ^a	AFBR-granule ^a	AFBR-biofilm ^a
			
Diameter (mm)	1.7 ± 0.9 (0.2–4.2) ^b	1.5 ± 0.3 (0.2–3.5)	1.8 ± 0.4 (1.0–2.6)
Roundness	2.6 ± 1.4 (1.2–10.4)	1.3 ± 0.5 (1.1–3.3)	1.6 ± 0.6 (1.3–2.6)
Settling velocity (m/h)	47 ± 18 (13–69)	64 ± 9 (21–78)	94 ± 15 (58–189)
Ash (%)	2.5 ± 0.5 (2.1–2.8)	8.6 ± 1.0 (8.3–9.4)	9.2 ± 1.0 (8.7–9.8)
ECP proteins (mg/g-VSS)	28 ± 3 (24–32)	29 ± 4 (26–35)	27 ± 4 (24–30)
ECP polysaccharides (mg/g-VSS)	152 ± 11 (145–169)	158 ± 9 (153–175)	154 ± 14 (142–174)

^aImages taken by the image analysis system.^bAverage ± standard deviation (measured range).

contents in the granules and biofilms were presumably attributed to the facts that synthetic glucose wastewater was fed wherein less inorganic materials were associated. Proteins contents in each gram of culture (in VSS) were 28 ± 3 mg ($n = 12$) in CSTR-granule, 29 ± 4 mg ($n = 12$) in AFBR-granule, and 27 ± 4 mg ($n = 12$), respectively; the corresponding contents of polysaccharides were found to be 152 ± 11 mg ($n = 12$), 158 ± 9 mg ($n = 12$), and 154 ± 14 mg ($n = 12$). Other ECP contents in the hydrogen-producing granules and biofilms, such as lipids, uronic acid and nucleic acids were not quantified, due to their small proportion in the hydrogen-producing granules as suggested by Fang et al. (2002).

SEM micrograph (Fig. 1A) revealed that rod-shaped microorganisms were found in the CSTR granules, having a length of $2.5\text{--}7\text{ }\mu\text{m}$ and a width of $0.4\text{--}0.6\text{ }\mu\text{m}$. Figure 1B illustrates the presence of cavities and holes among the immobilized bacterial clusters. The cavities may allow substrate, metabolic products as well as the release of biogas to be efficiently transferred. Similar bacterial morphologies and structural properties were exhibited by other granules and biofilms, which were not presented here for brevity.

Microbial Species Analysis

Bacterial community analysis using DGGE techniques is based on the separation of PCR-amplified same length fragments of genes coding for 16S rDNA. Each band on the DGGE profiles corresponded to a gene fragment of unique 16S rDNA sequences and accordingly represented a specific species in the microbial community, whereas the intensity of a band represents the relative abundance of the corresponding microbial species (Fang and Liu, 2002; Zhang and Fang, 2001). The DGGE profiles (data not shown) show a distinctly distinguishable band present in each microbial community as DNA fragments were amplified with different sets of primers. In addition, the bands corresponding to

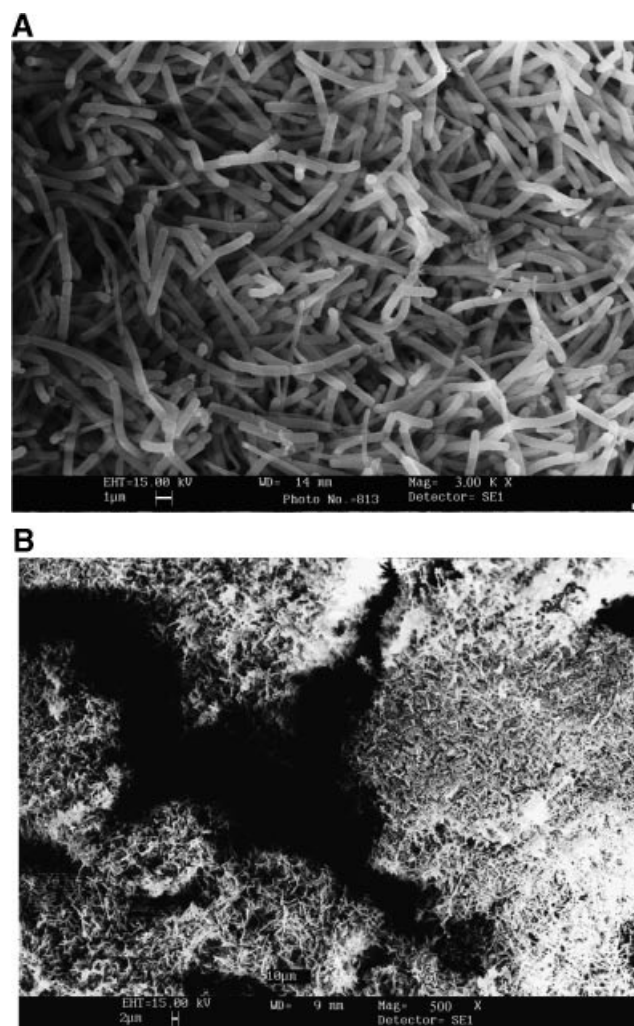
**Figure 1.** SEM photographs of (A) typical surface bacterial morphology and (B) porous structure of hydrogen-producing bioparticles.

Table IV. Phylogenetic affiliation of bacterial sequences.

Culture type	Number of bases used in establishing identity	Phylogenetic relationship	
		Closest species in GenBank	Similarity (%)
CSTR-granule	1,350	<i>Clostridium pasteurianum</i> (CH7)	98
AFBR-granule	1,359	<i>C. pasteurianum</i> (CH4)	98
AFBR-biofilm	1,401	<i>C. pasteurianum</i> (CH7)	98

different samples appeared at the same location of DGGE profiles, indicating a similar microbial composition of the different microbial communities. The PCR-amplified DNA genes were sequenced and the obtained sequences were compared with those of the reference microorganisms available in the GenBank database by BLAST search. All bacterial sequences were found to be most closely related to the bacterial species of *Clostridium pasteurianum* with similarities of 98% (Table IV). Figure 2 illustrates that the phylogenetic tree for three bacterial strains designed as CSTR-G, AFBR-G and AFBR-B were closely related to the *Clostridium* species.

CLSM Images

Figures 3 and 4 show the confocal images of the 40 μ m section, scanned at 360 μ m from the outer surface of a hydrogen-producing granule or biofilm by detecting the distribution of proteins, α -polysaccharides, β -polysaccharides, lipids, dead cells and living cells. Proteins were distributed uniformly in the healthy granules (Figs. 3A

and 4A) and biofilm (Fig. 4B), while other ECP contents (polysaccharides and lipids) and cells were mostly accumulated on the outer layer of granules or biofilms. Deeper inside the granule was a core made mainly of proteins. High bioactivity in the outer layer was expected. Unlike the layer structure of healthy granules, “patch flocs” had a uniform structure as cells and ECP contents were distributed relatively evenly in the granule’s interior (Fig. 3B). This uniform structure might be caused by the presence of small pores as detected in the granule interior (Fig. 4B), which could be functioned as mass transfer channels for the contact between substrate and microbial cells.

Discussion

Although the sizes of granule cultivated in the CSTR and AFBRs were comparable, the granule shapes were quite different, as evidenced by their roundness. Violent shear forces from the stirring impellers of the CSTR made the granules disintegrated and amorphous, while moderate liquid shear force kept granules more uniform in shape in

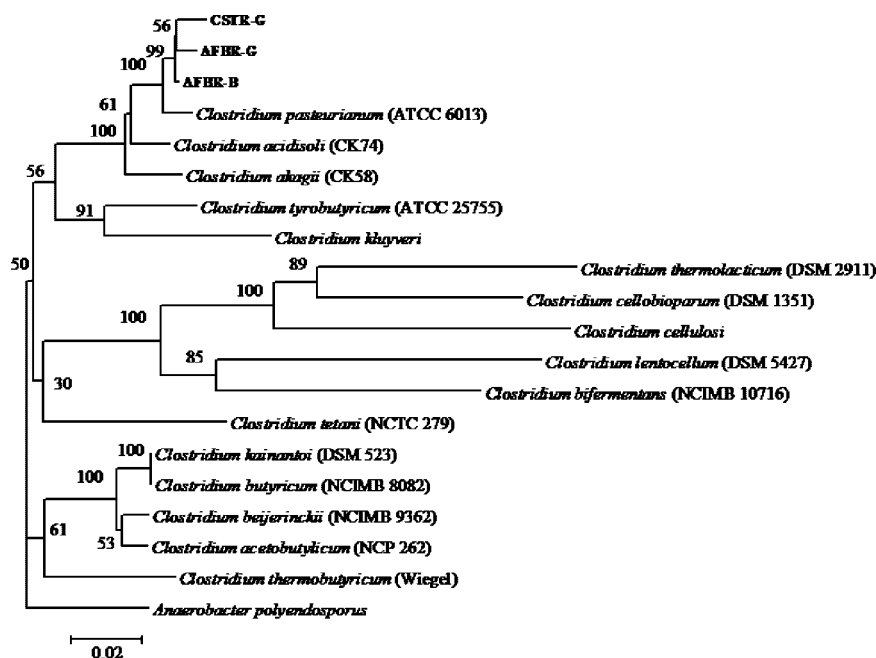


Figure 2. 16S rDNA phylogenetic tree for stains CSTR-G, AFBR-G and AFBR-B, and their close relatives in species *Clostridium*. The tree is based on the Jukes-Cantor distance and was constructed using a neighbor-joining algorithm with 500 bootstrappings. *Anaerobacter polyendosporus* was selected as the outgroup species. The scale bar represents 0.02 nucleotide divergence. Numbers at the nodes are the bootstrap values (%). Nucleotide sequence accession numbers or stain names are indicated in brackets.

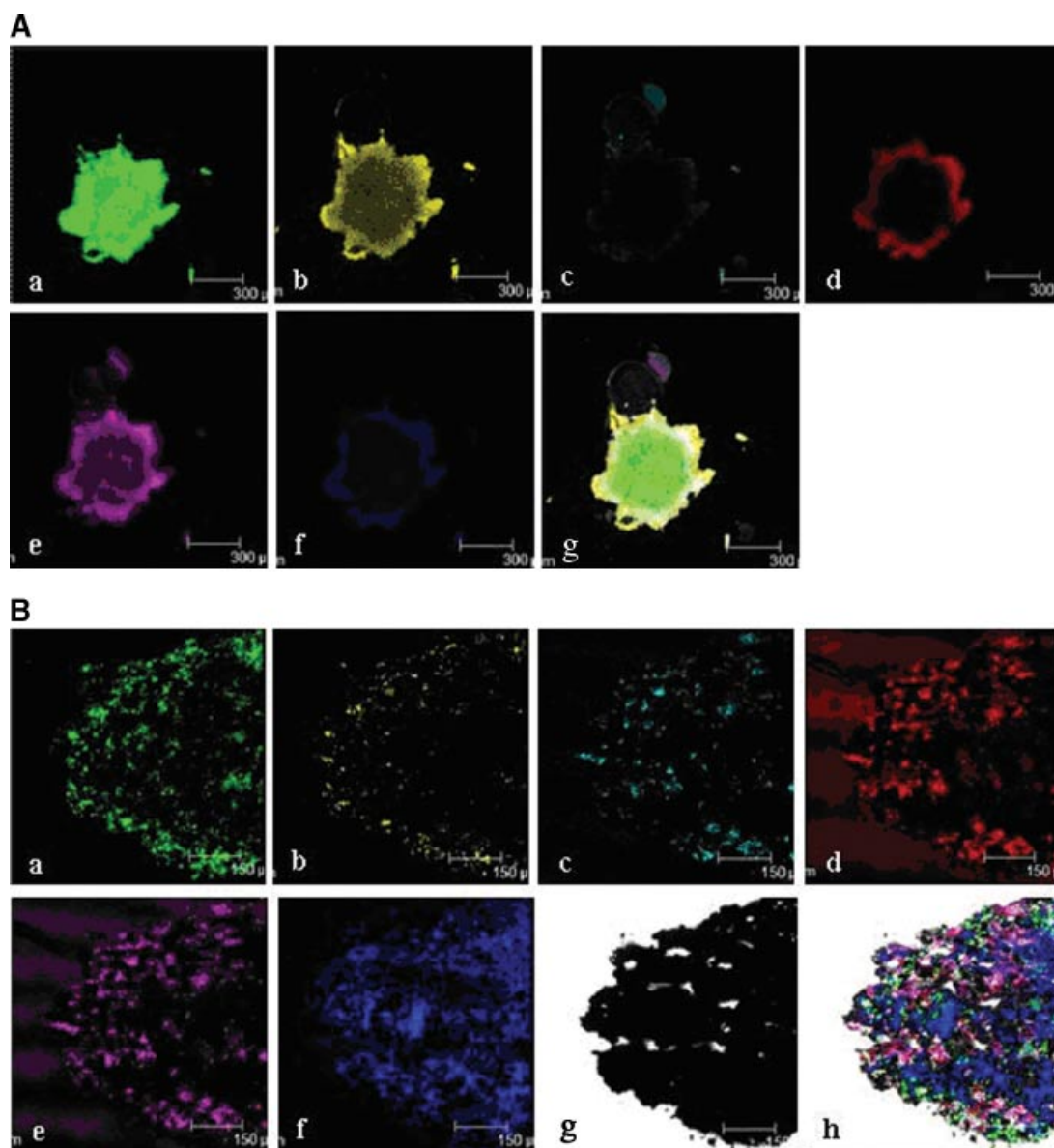


Figure 3. Confocal images of hydrogen-producing granules cultivated in the CSTR: (A) healthy granule and (B) patch flocs. Green: proteins (a); yellow: lipids (b); light blue: α -polysaccharides (c); red: living cells (d); pink: dead cells (e); blue: β -polysaccharides (f); light background: microscopic image (g); Last figure: merging of all (6 or 7) images (g/h). [Color figure can be seen in the online version of this article, available at www.interscience.wiley.com.]

the AFBRs. The biofilm particles also displayed a uniform shape despite the irregular shape of GAC carriers under moderate shear force. The settling velocities of biofilms were substantially higher than those of granules, and granules cultivated in the AFBR had a better settling ability compared to the CSTR granules. These findings indicate that column reactors seem to be favorable for the solid–liquid separation and biomass retention of hydrogen-producing biofilms and granules. Granule physical properties, such as granule size and settling velocities presented in the present study are consistent with those found for normal hydrogen-producing granules or bioflocs (Fang et al., 2002; Mu and Yu, 2006; Zhang et al., 2004).

Bacterial morphology of the bioparticles cultivated in the present study appeared to be very uniform. The microbial community of the granules or biofilms was uniquely constituted by the rod-shaped hydrogen-producing bacteria, which were identified to be *C. pasteurianum* by analyzing their nucleotide sequences (Fig. 1a). The simple microbial composition of sludge samples tested was most likely attributed to the fact that only one predominant species was found in the acclimated seed sludge (Zhang et al., 2006). Previous studies indicated that filamentous, fusiform-like and coccus-like bacteria were also present in the hydrogen-producing granules (Fang et al., 2002; Mu and Yu, 2006; Wu et al., 2006). Different mixed-cultures

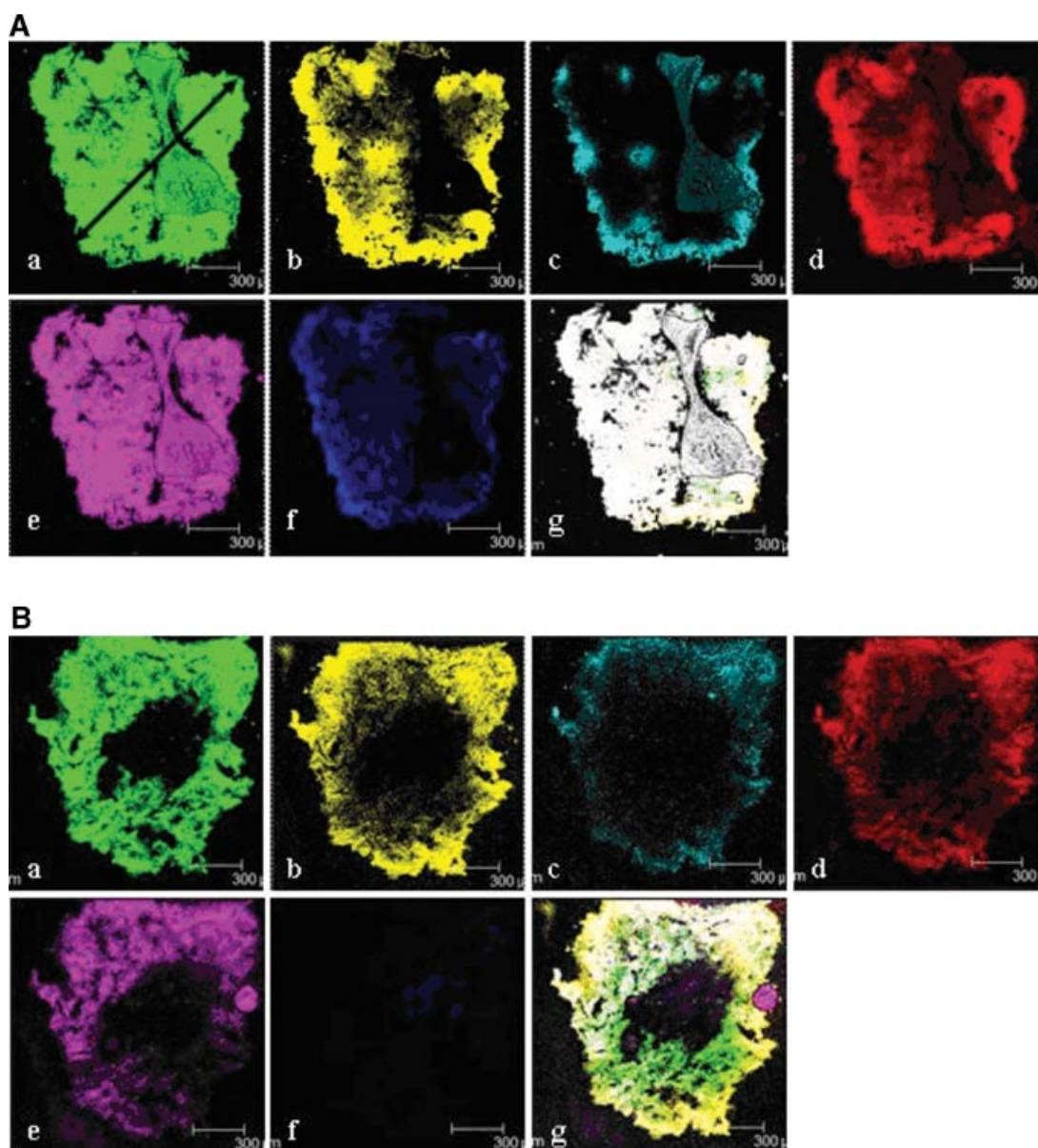


Figure 4. Confocal images of hydrogen-producing granules (A) and biofilms (B) cultivated in the AFBRs. Green: proteins (a); yellow: lipids (b); light blue: α -polysaccharides (c); red: living cells (d); pink: dead cells (e); blue: β -polysaccharides (f). Last figure: merging of all (6) images (g). [Color figure can be seen in the online version of this article, available at www.interscience.wiley.com.]

were used as the seed sludge in those studies, which might contribute to the relatively complex microbial composition. It is interesting to note that *C. pasteurianum*-like bacterium (similarity, 98%) was also found to be unique microbial species in the self-flocculated hydrogen-producing granules, but exhibited a fusiform shape (3–5 μm in length and 1–2 μm in width) (Wu et al., 2006). Such an inconsistency in cell shape might result from the different operating conditions as the granules were cultivated by Wu et al. (2006) with sucrose in a CSTR at 40°C and pH 6.6 ± 0.2 .

The physical and structural properties of particle-supported biofilms and granules were similar, as were their microbial composition and distribution. Living cells

were mostly accumulated on the outer layer of granules, while deeper inside of the granules was a core made of less active cells and mainly of ECP. Therefore, particle-supported biofilms and granules will be considered as a single category: particle-based biofilms. In fact, a comparable hydrogen production performance in terms of hydrogen yield and specific hydrogen production rate was demonstrated by the granular sludge and biofilms. Their microbial conversion efficiency of glucose to hydrogen, evaluated on the basis of a maximum of 4 mol- H_2 /mol-glucose, varied in a narrow range from 41.5% to 45.3%, which were compared well with the values previously reported (Fang et al., 2002; Liu and Fang, 2003; Wu et al., 2006). Nevertheless, specific hydrogen production

rates of the immobilized sludge, that is, granules and biofilms were nearly half of that of suspended sludge (15.62 mmol- H_2 /g-VSS h). This indicates that, although numerous pores existed within the granules or biofilms, a large amount of ECP secreted might clog up these pores and hence reduced the mass transfer capability through the bioparticle interior, as evidenced by the presence of numerous dead cells throughout the granules or biofilms.

The phylogenetic tree revealed that strains CSTR-G and AFBR-G clustered closely with strain AFBR-B, as indicated by a high bootstrap value of 99% (Fig. 2). These three strains further formed a very compact phylogenetic cluster with *C. pasteurianum*, and this relationship was robust, as supported by a bootstrap value of 100%. The sequence identities between the three strains were found to be larger than 99%, indicating that strains AFBR-G, CSTR-G and AFBR-B were very closely related and might be distinguishable at the strain level. *C. pasteurianum* is a classic volatile fatty acids (mainly, butyrate and acetate) and hydrogen producer, and its growth might be stimulated by the fermentable carbohydrate, such as sucrose and glucose (Dabrock et al., 1992).

It is interesting to note that bacterial species *C. pasteurianum*-like were found predominant in two recent reports studying on the microbial community of hydrogen-producing granules. Wu et al. (2006) found that bacterial compositions in a hydrogen-producing reactor became simple and a shift of microbial population occurred as the HRT decreased from 6 to 0.5 h. Self-flocculated granules were formed as the HRT was shortened to 0.5 h, at which a unique bacterial species was detected by PCR-DGGE analysis whose sequence was found to be highly similar (98% similarity) to that of an uncultured *C. pasteurianum* strain. It should be realized that this bacterial strain was not found before the formation of self-flocculated granules. Fang et al. (2002) also found that 46.2% of the clones derived from hydrogen-producing granules were most closely related to *C. pasteurianum* with a similarity of 94–96%. These findings seem to indicate that *C. pasteurianum* or the strains close to *C. pasteurianum* might be the crucial microbial species participating in the formation of hydrogen-producing granules.

It follows that microbial population and ECP are likely to play important roles in the formation of granules. A common viewpoint postulates that filamentous bacteria might be favorable for the microbial immobilization of anaerobes (Macleod et al., 1990; Morgan et al., 1991). For example, Wiegant (1998) observed that steady granules could be developed from the precursors mainly containing filamentous *Methanosaeta* in UASB reactors. Initially, *Methanosaeta* form very small aggregates via bridging between microbial cells or microflocs, or attaching to finely dispersed matter. Cellular multiplication and entrapment of non-attached bacteria lead to the growth of the precursors to form granules. Because of the absence of filamentous structure, however, *Methanosarcina*, typical coccoid methanogens, are believed to form granules through secreting

much more ECP compared to *Methanosaeta* and thus form clumps of bacteria (Chen and Lun, 1993). *Methanosarcina* are responsible for the nucleus formation as the anaerobic cultures are fed with acetate, especially at the high organic loading rates (Bochem et al., 1982; Wu et al., 1996). The granules are developed as the clumps reach macroscopic dimensions and other species, such as *Methanosaeta* tend to inhabit in the *Methanosarcina* clumps.

C. pasteurianum is a nonhomoacetogenic hydrogen-producing species present either singly or in pairs and excretes intracellular polysaccharide reserve (Fang et al., 2002). Like *Methanosarcina*, *C. pasteurianum*-like bacterium is lack of filamentous structure. Secreting ECP might favor the formation of *C. pasteurianum* granules. It has been known that ECP has a high affinity to attach to substratum surface, such as microbial cells and carrier materials (Cogan and Keener, 2004; Liu et al., 2004; Schmidt and Ahring, 1996). In that case, ECP would serve as a bio-glue to facilitate *Clostridium* interaction and further strengthen hydrogen-producing aggregate structure through formation of a polymeric network. It should be noted that since most of the centre of the aggregates consisted of dead cells, a bigger granule may not necessarily bring about better performance. It appears that granulation may strengthen the biomass structure, but in some instances may had lower hydrogen production than the acclimated sludge (Table II).

The ECP in hydrogen-producing granules and biofilms consisted mainly of proteins and polysaccharides, approximately in a ratio of 0.2:1 ($n = 12$). This finding is in consistent with the reported ranges between 0.2:1 and 0.6:1 (Fang et al., 2002; Mu and Yu, 2006). On the other hand, relatively high ratios of proteins to polysaccharides ranging from 2:1 to 6:1 were reported for methanogenic granules (Schmidt and Ahring, 1996). Some researchers pointed out that, unlike the significant role played by proteins in methanogenic granulation, polysaccharides might be the key ECP constituent in the formation of hydrogen-producing granules (Fang et al., 2002; Mu and Yu, 2006). The role of ECP in the microbial granulation had been noted previously (Hulshoff Pol et al., 2004; Liu et al., 2004). It had been found that the acid incubation did stimulate the production of ECP proteins, and accelerated the process of granulation (Zhang et al., 2007a,b). Zhang et al. (2007b) noted that the total increments of proteins and polysaccharides during the 24-h acid incubation were estimated to be about 27.5 and 18.0 mg/L, respectively. While almost all of the protein was attached on the microbial cells, only about 67% of the increased polysaccharides were found on the cellular surface. This led to an increased ratio of proteins to polysaccharides of microbial culture from 0.2 to 0.5–0.8. In addition, microbial aggregates that could be considered as the initial nuclei had appeared by the end of the acid incubation. As shown in Figures 3A and 4A, proteins were distributed uniformly over the granule interior in contrast to other ECP contents. These findings indicated that ECP proteins might play an important role in the initial stage of granulation of hydrogen-producing culture. In other word, microbial

aggregation of hydrogen-producing culture may start as a protein-rich matrix or nucleus has been established. The protein matrix might contain microbial cells and proteins that could be enriched by secretion of the attached cells or by entrapping extraneous proteins in a form of macromolecules, colloids and slimes. In fact, a lower accumulation rate of ECP proteins was found under normal conditions without the acidification and a much longer period of granulation of hydrogen-producing culture was required (Zhang et al., 2007a).

Conclusions and Recommendations

Phylogenetic analysis indicated that a pure culture of *C. pasteurianum*-like bacterium was found in microbial community of rapidly formed hydrogen-producing granules and biofilms. It is postulated that containing such a species favored the rapid immobilization of hydrogen-producing culture. The high productivity of ECP, a bio-glue to facilitate cell-to-cell and/or cell-to-substratum interaction, may work as the driving forces for the immobilization of *C. pasteurianum*. As abundant proteins were noted in the granule cores, it can be derived that rapid formation of the hydrogen-producing granules could be due to the establishment of precursor protein-rich microbial nuclei.

The phylogenetic analysis showed that microbial diversity between CSTR-granules, AFBR-granules and AFBR-biofilms was quite similar and only distinguishable in a strain level. Microbial mutation may occur. Gene cloning and structural analysis plus physiological characterization may be conducive to identifying and distinguishing those bacterial strains.

Although the sizes of granules and biofilms were measured in the present study, the size effect on hydrogen production rate was not investigated. Because of most living cells locating outside of particles, smaller granules or thinner biofilms might enhance the hydrogen production efficiency. One challenge remains here is the control of biofilm thickness and granule size.

The authors would like to acknowledge Dr. Xiaoge Chen for her technical direction and software operation in the phylogenetic analysis of microbial population.

References

- Adav SS, Chen MY, Lee DJ, Ren NQ. 2007. Degradation of phenol by aerobic granules and isolated yeast *Candida tropicalis*. *Biotechnol Bioeng* 96(5):844–852.
- APHA. 1998. Standard methods for the examination of water and wastewater. Washington, DC, USA: American Public Health Association.
- Aquino SF, Stuckey DC. 2003. Production of soluble microbial products (SMP) in anaerobic chemostats under nutrient deficiency. *J Environ Eng-ASCE* 129(11):1007–1014.
- Bochem HP, Schoberth SM, Sprey B, Wengler P. 1982. Thermophilic biomethanation of acetic acid—morphology and ultrastructure of a granular consortium. *Can J Microbiol* 28(5):500–510.
- Chen J, Lun SY. 1993. Study on mechanism of anaerobic sludge granulation in UASB reactors. *Water Sci Technol* 28(7):171–178.
- Chen MY, Lee DJ, Tay JH. 2007a. Distribution of extracellular polymeric substances in aerobic granules. *Appl Microbiol Biotechnol* 73:1463–1469.
- Chen MY, Lee DJ, Tay JH. 2007b. Staining of extracellular polymeric substances and cells in bio-aggregates. *Appl Microbiol Biotechnol* 75:467–474.
- Cogan NG, Keener JP. 2004. The role of the biofilm matrix in structural development. *Math Med Biol: J IMA* 21(2):147–166.
- Dabrock B, Bahl H, Gottschalk G. 1992. Parameters affecting solvent production by *Clostridium pasteurianum*. *Appl Environ Microbiol* 58(4):1233–1239.
- Dubois M, Gilles KA, Hamilton JK, Rebers PA, Smith F. 1956. Colorimetric method for determination of sugars and related substrates. *Anal Chem* 28(3):350–356.
- Fang HHP, Liu H. 2002. Effect of pH on hydrogen production from glucose by a mixed culture. *Bioresour Technol* 82(1):87–93.
- Fang HHP, Liu H, Zhang T. 2002. Characterization of a hydrogen-producing granular sludge. *Biotechnol Bioeng* 78(1):44–52.
- Felsenstein J. 1989. PHYLIP (PHYlogenetic Inference Package). *Cladistics* 5:164–166.
- Hall TA. 1999. BioEdit: A user-friendly biological sequence alignment, editor and analysis program for Windows 95/98/NT. *Nucleic Acids Symp Ser* 41:95–98.
- Hulshoff Pol LW, de Castro Lopes SI, Lettinga G, Lens PNL. 2004. Anaerobic sludge granulation. *Water Res* 38(6):1376–1389.
- Liu H, Fang HHP. 2002. Extraction of extracellular polymeric substances (EPS) of sludges. *J Biotechnol* 95(3):249–256.
- Liu H, Fang HHP. 2003. Hydrogen production from wastewater by acidogenic granular sludge. *Water Sci Technol* 47(1):153–158.
- Liu YQ, Liu Y, Tay JH. 2004. The effects of extracellular polymeric substances on the formation and stability of biogranules. *Appl Microbiol Biotechnol* 65(2):143–148.
- Macleod FA, Guiot SR, Costerton JW. 1990. Layered structure of bacterial aggregates produced in an upflow anaerobic sludge bed and filter reactor. *Appl Environ Microbiol* 56(6):1598–1607.
- Maidak BL, Cole JR, Lilburn TG, Parker CTJ, Saxman PR, Stredwick JM, Garrity GM, Li B, Olsen GJ, Pramanik S, Schmidt TM, Tiedje JM. 2000. The RDP (Ribosomal Database Project) continues. *Nucleic Acids Res* 28:173–174.
- Morgan JW, Evison LM, Forster CF. 1991. The internal architecture of anaerobic sludge granules. *J Chem Technol Biotechnol* 50(2):211–226.
- Mu Y, Yu HQ. 2006. Biological hydrogen production in a UASB reactor with granules. I. Physicochemical characteristics of hydrogen-producing granules. *Biotechnol Bioeng* 94(5):980–987.
- Muyzer G, de Waal E, Uitterlinden A. 1993. Profiling of complex microbial populations by denaturing gradient gel electrophoresis analysis of polymerase chain reaction-amplified genes coding for 16S rRNA. *Appl Environ Microbiol* 59(3):695–700.
- Oh YK, Kim SH, Kim MS, Park S. 2004. Thermophilic biohydrogen production from glucose with trickling biofilter. *Biotechnol Bioeng* 88(6):690–698.
- Schmidt JE, Ahring BK. 1996. Granular sludge formation in upflow anaerobic sludge blanket (UASB) reactors. *Biotechnol Bioeng* 49(3):229–246.
- Show KY, Zhang ZP, Tay JH, Liang DT, Lee DJ, Jiang WJ. 2007. Production of hydrogen in a granular sludge-based anaerobic continuous stirred tank reactor. *Int J Hydrogen Energy* 32(18):4744–4753.
- Wiegant WM. 1998. The Spaghetti theory on anaerobic granular sludge fermentation. *Proceeding of the granular anaerobic sludge*; Wageningen. p 146–152.
- Wu WM, Jain MK, Zeikus JG. 1996. Formation of fatty acid-degrading, anaerobic granules by defined species. *Appl Environ Microbiol* 62(6):2037–2044.
- Wu SY, Hung CH, Lin CN, Chen HW, Lee AS, Chang JS. 2006. Fermentative hydrogen production and bacterial community structure in high-rate anaerobic bioreactors containing silicone-immobilized and self-flocculated sludge. *Biotechnol Bioeng* 93(5):934–946.

- Yu HQ, Mu Y. 2006. Biological hydrogen production in a UASB reactor with granules. II. Reactor performance in 3-year operation. *Biotechnol Bioeng* 94(5):988–995.
- Zhang T, Fang HH. 2001. Phylogenetic diversity of a SRB-rich marine biofilm. *Appl Microbiol Biotechnol* 57(3):437–440.
- Zhang JJ, Li XY, Oh SE, Logan BE. 2004. Physical and hydrodynamic properties of flocs produced during biological hydrogen production. *Biotechnol Bioeng* 88(7):854–860.
- Zhang ZP, Show KY, Tay JH, Liang DT, Lee DJ, Jiang WJ. 2006. Effect of hydraulic retention time on biohydrogen production and anaerobic microbial community. *Process Biochem* 41(10):2118–2123.
- Zhang ZP, Show KY, Tay JH, Liang DT, Lee DJ. 2007a. The role of acid incubation in rapid immobilization of hydrogen-producing culture in anaerobic upflow column reactors, Daejeon: Korea.
- Zhang ZP, Show KY, Tay JH, Liang DT, Lee DJ, Jiang WJ. 2007b. Rapid formation of hydrogen-producing granules in an anaerobic continuous stirred tank reactor induced by acid incubation. *Biotechnol Bioeng* 96(6):1040–1050.
- Zhang ZP, Tay JH, Show KY, Yan R, Liang DT, Lee DJ, Jiang WJ. 2007c. Biohydrogen production in a granular activated carbon anaerobic fluidized bed reactor. *Int J Hydrogen Energy* 32(2):185–191.
- Zhang Z-P, Show K-Y, Tay J-H, Liang DT, Lee D-J. 2008a. Biohydrogen production with anaerobic fluidized bed reactors—A comparison of biofilm-based and granule-based systems. *Int J Hydrogen Energy* 33(5):1559–1564.
- Zhang ZP, Show KY, Tay JH, Liang DT, Lee DJ. 2008b. Enhanced continuous biohydrogen production by immobilized anaerobic microflora. *Energy Fuels* 22:87–92.